Photofabrication of Surface Relief Grating on Films of Azobenzene Polymer with Different Dye Functionalization

Takashi Fukuda* and Hiro Matsuda

Department of Polymer Chemistry, National Institute of Materials and Chemical Research (NIMC), 1-1 Higashi, Tsukuba 305-8565, Japan

Takao Shiraga, Tatsumi Kimura, and Masao Kato

Department of Materials Science and Technology, Science University of Tokyo, 2641 Yamazaki, Noda 278-8510 Japan

Nirmal K. Viswanathan, Jayant Kumar, and Sukant K. Tripathy

Center for Advanced Materials, University of Massachusetts Lowell, Lowell, Massachusetts 01854

Received October 26, 1999; Revised Manuscript Received March 20, 2000

ABSTRACT: Photofabrication of surface relief grating (SRG) on very high-T_g and lower-T_g azobenzene functionalized polymers was investigated. Polymers with different degrees of functionalization were designed and synthesized to understand the chemical and physical intricacies involved at the molecular level in the photofabrication of SRG. The systematic study examined the influence of three important parameters: the degree of azo functionalization, the irradiating light intensity, and the initial film thickness. From the experimental results, we establish that the writing behavior of photofabricated SRG depends on the degree of azo functionalization. The effective critical intensity of the irradiating light was found to be independent of the degree of functionalization. Threshold behavior for the deformation process as a function of the degree of functionalization was established. The observed film thickness dependence of the SRG formation is discussed within the framework of existing fluid mechanics model. The thermal properties of the photofabricated SRG were also investigated.

Introduction

Azobenzene functionalized polymers are interesting and potentially useful materials for optical device applications. The photoanisotropic azobenzene molecules upon irradiation with polarized light show photoinduced reorientation through the trans−cis−trans photoisomerization cycles. This reorientation also forms the primary step in the light-induced mass transport process, observed in azobenzene functionalized polymer films. Photofabrication of surface relief gratings (SRG) on thin azobenzene functionalized polymer films utilizing this mass transport process has recently attracted great attention.[1−12] The SRGs with large modulation depth are unique to the azobenzene functionalized polymer systems, and the process is quite different from other conventional microscopic processing techniques such as laser ablation and chemical etching. The major advantage of this photofabrication approach is the facile one-step procedure and the fact that the modulation depth can be precisely controlled by adjusting the light exposure time and the polarization states of the writing beam. This kind of photofabrication on polymer films promises to be an effective and simple solution to assemble an optoelectronic integrated circuit. This phenomenon is also interesting from the standpoint of fundamental polymer photophysics, because the SRGs are formed as a result of large-scale photodriven mass transport process in thin solid films at a temperature much below the T_g of the polymer.

In recent years, there have been many discussions about the mechanism of this phenomenon, and some models have been suggested.[13−16] According to Kumar et al, the origin of the driving force is derived from the dipolar interaction of the azo chromophores with the optically induced electric field gradient.[13] In addition, it is experimentally verified that the SRG formation process is initiated at the film surface and continues through the bulk of the material as polymer layers are moved.[8] Deformation behavior and surface modulation profiles had been successfully simulated on the basis of this model using only one molecular level viscosity parameter.[10] Barrett et al. have proposed a model based on the internal pressure caused by the free volume expansion driven by the photoisomerization process. The process is suggested to be a result of bulk deformation and is described by the Navier−Stokes equations for laminar flow of viscous fluid.[14] A mean-field theory of photoinduced SRG formation in liquid crystalline azo functionalized polymer films has been presented by Pedersen et al.[15] Recently, Sumaru et al. have further extended the fluid mechanics model appropriately incorporating the depth dependence of driving force considering light attenuation in the film and discussed the dynamics of photoinduced SRG formation as a function of initial film thickness.[16]

We have been interested in establishing a relationship between the observed deformation features, aspects of the molecular photodynamics, and the molecular level structural parameters. A number of new insights into the fabrication dynamics were established on the basis of our recent investigation of the photofabrication of SRG on maleimide-based high-T_g (170−279 °C) polymers with different degrees of azobenzene functionalization.[18] Surface modulation of the photofabricated SRG was found to depend on the degree of azo functionalization. While the formation of SRG is a dose-dependent process, a minimum threshold intensity of irradiating light is necessary to initiate the process, and

10.1021/ma991803d CCC: $19.00
Published on Web 05/03/2000

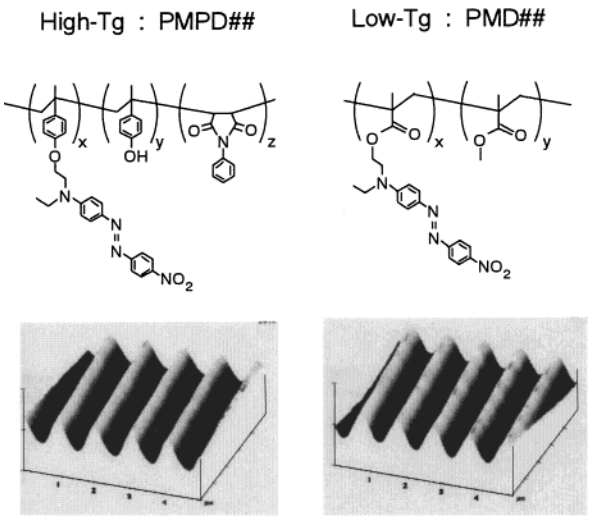

Figure 1. Chemical structure of high-T_g polymers (left: PMPD) and low-T_g polymers (right: PMD). The insets are the typical AFM images of each polymer. The dimensions and the surface modulations of the both AFM images are 5 × 5 μm and about 100 nm, respectively. The numbers following the abbreviation of polymer (PMPD and PMD) indicate the degree of functionalization of the polymer.

this minimum threshold intensity does not depend on the degree of functionalization of the polymer. Finally, the temperature dependence of the SRG inscription rate was found to be independent of the degree of functionalization.

In this paper, we have carried out a systematic study of the deformation process on lower-T_g (∼120 °C) azobenzene functionalized polymers. The photofabrication properties of the high- and low-T_g azobenzene polymers with different degrees of functionalization are compared. The general behavior in both the polymer systems is discussed regarding the functionalization dependence of SRG photofabrication process and the minimum threshold for irradiating light to inscribe the SRGs effectively. The film thickness dependence of the SRG formation process is discussed within the framework of the previously proposed extended fluid mechanics model.

Experimental Section

High-T_g Polymer Synthesis. A prepolymer (alternating copolymer) was obtained by copolymerization of isopropenylphenol and *N*-phenylmaleimide in THF with the use of azobis(isobutyronitrile) (AIBN) as a radical initiator. The reaction mixture was allowed to stand at 60 °C for 24 h. The residue was precipitated from methanol as a white powder with an 81% yield. Molecular weight was estimated by gel permeation chromatography to be $M_n = 1.5 \times 10^4$ by use of a PS calibration and $M_w/M_n = 1.6$. ^{1}H NMR (DMSO-d_6): d = 6.3−7.6 (m, 9H, aromatic H), 9.2−9.6 (br, 1H, OH). Comparing the gross area, the copolymerization ratio of isopropenylphenol to *N*-phenylmaleimide was found to be 0.52:0.48. The polymer was post modified to a copolymer of 4′-[*N*-ethyl-*N*-(4-isopropenylphenoxyethyl) amino]-4″-nitroazobenzene and *N*-phenylmaleimide by a polymer reaction of Mitsunobu coupling with Disperse Red 1 (DR-1). Details of this synthesis have been reported in the literature.[19] The chemical structure of the copolymer (PMPD) and the typical profile of the SRG fabricated on a PMPD film are shown in Figure 1. The degree of azobenzene functionalization of PMPD could be changed by the amount of DR-1 in the reaction mixture and the reaction time. The degree of functionalization was defined as the ratio of the formula weight of the azo chromophore to that of the whole molecule. It was estimated from the absorption spectrum and NMR. Hereafter, each PMPD sample will be referred to as PMPD##, where ## is the degree of dye functionalization. PMPD having four different dye functionalizations were synthesized for this work. A differential scanning calorimeter (DSC) was used to measure the glass transition temperature (T_g) of the polymers.

Low-T_g Polymer Synthesis. A monomer material of 4-(*N*-(2-methacryloyloxyethyl)-*N*-ethylamino)-4′-nitroazobenzene (DR-1MA) was obtained by a coupling of 4-[*N*-(2-hydroxyethyl)-*N*-ethylamino]-4′-nitroazobenzene and methacryloyl chloride. The reaction mixture was allowed to stand at room temperature for 2 h. The residue was recrystallized from methanol to obtain red crystal; mp = 94.6−95.1 °C with a yield of 31.5%. A low-T_g polymer (PMD) shown in Figure 1 was obtained by copolymerization of DR-1MA and methyl methacrylate. The synthesis of this kind of copolymer has already been reported.[20] A typical surface profile of the SRG fabricated on a PMD film is also shown in the figure. The degree of azobenzene functionalization of PMD could be changed by the stoichiometry of DR-1MA in the reaction mixture and the reaction time. In the same manner as for the high-T_g polymer (PMPD), the degree of functionalization was defined by the weight ratio of the azo chromophore. It was also estimated from the absorption spectrum and NMR. Hereafter, each PMD sample will be referred to as PMD##, where ## is the degree of dye functionalization. PMD having seven different dye functionalization levels were synthesized. Again a DSC was used to measure the T_g's of these polymers.

Sample Preparation. The copolymers are dissolved in dichloromethane or chloroform, and the polymer solutions were filtered by mesh filter with 0.2 μm pore. Amorphous thin films with good optical quality were prepared on glass substrates by spin coating. The films were dried in a vacuum for more than 12 h. The thickness of the films was measured using a mechanical stylus profiler and confirmed by the optical prism coupling technique (Metricon 2010).

Optical Arrangement. The optically induced surface relief grating was recorded by exposing the polymer thin film sample to an interference pattern. The interference pattern was produced by the two coherent beams at 488 nm from an Ar^+ laser with intensities ranging from 2 to 100 mW/cm^2. The details of the optical arrangement were previously reported.[2] Laser intensities given in this report were measured just after the collimating lens. The angle between the two incident beams was selected to be 14°, resulting in the line spacing of approximately 1 μm in the interference pattern. The polarization of the two beams was selected to be circular (RCP:LCP) or linear (+45°:−45°) which was defined as the angle between the two polarization with respect to s-polarization. The diffraction efficiency of the first-order diffracted beam from the surface gratings in transmission mode was probed with an unpolarized low power He−Ne laser beam at 632.8 nm. Although the PMPD and PMD polymers have a weak absorption at a wavelength of 632.8 nm, the absorption was taken into account for a calculation of the diffraction efficiency. The probe beam was incident at normal to the surface of the polymer film.

Surface Analysis. The surface structure of the gratings on the PMPD and the PMD polymer films were investigated by atomic force microscopy (AFM, Nanoscope IIIa, Digital Instruments Co.) in the tapping mode under ambient conditions.

Results and Discussion

Four kinds of PMPD and seven kinds of PMD with different azobenzene functionalization were synthesized. The characterization details of each polymer are listed in Table 1.

The functionalization dependence of SRG formation on high-T_g (PMPD) and lower-T_g (PMD) polymers is shown in Figure 2. SRG was fabricated on each polymer film with different functionalization at the same photon dose, i.e., the same light intensity and the same

Table 1. Characterization of Each Polymer[a]

PMPD			PMD		
func (wt %)	T_g (°C)	M_n	func (wt %)	T_g (°C)	M_n
46	170	2.7×10^4	78	125	4.5×10^3
40	176	2.5×10^4	76	130	7.8×10^3
35	232	2.2×10^4	72	132	1.2×10^4
18	279	1.8×10^4	53	128	5.9×10^3
0	>300	1.5×10^4	39	130	1.2×10^4
			27	119	6.9×10^3
			15	125	1.6×10^4
			0	110	1.2×10^4

[a] T_g = glass transition temperature; M_n = number-averaged molecular weight.

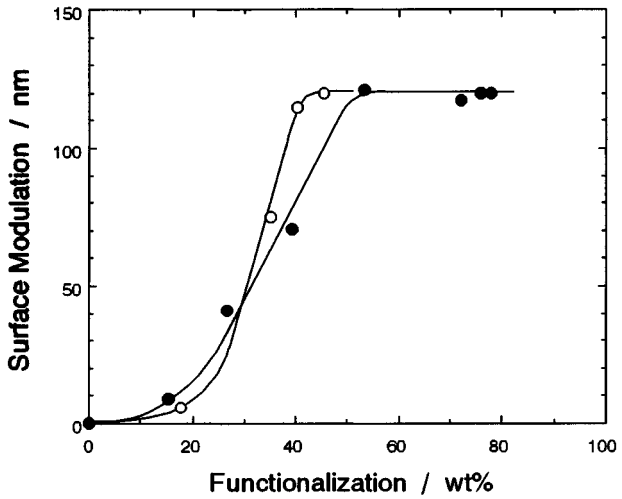

Figure 2. Functionalization dependence of the SRG inscription rate. Open and closed circles correspond to high-T_g PMPD and low-T_g PMD, respectively. The surface modulation (vertical axis) was measured by AFM after a certain photon dose (600 J/cm^2 for PMPD and 18 J/cm^2 for PMD).

exposure time. The surface modulation obtained at the same photon dose can be represented by an S-shaped curve for both high-T_g (PMPD) and low-T_g (PMD) azo polymers. This result suggests that the effective SRG inscription rate depends on the number of azobenzene chromophore attached to the polymer molecules below a certain functionalization point (Φ = 40−50 wt %). Above this threshold degree of functionalization, however, the inscription rate is independent of the degree of functionalization.

From the microscopic viewpoint, the degree of functionalization is directly related to the separation between the neighboring dye chromophores, which dictates the kinetics of the system because the mass transporting force acts on the macromolecular chains through the azo chromophores. The saturation point appears to shift to a higher degree of functionalization for the higher-T_g polymers, which may due to the rigidity of the main chain. It should be noted that deep surface modulation could still be formed even on very low functionalized azo polymers if the sample is exposed for a higher photon dose. For example, 100 nm depth SRG could be fabricated on 1.0 μm thick PMD 15 after the irradiation of 149 J/cm^2 (with 40 mW/cm^2 light) and 10 nm depth SRG on 1.0 μm thick PMPD18 after a dose of 368 J/cm^2 (with 50 mW/cm^2 light), respectively.

One of the reasons for the saturation of the SRG inscription rate in the higher azo functionalization region is attributable to the effects of light absorption. As the absorption coefficient of the sample is proportional to the degree of functionalization, the penetration

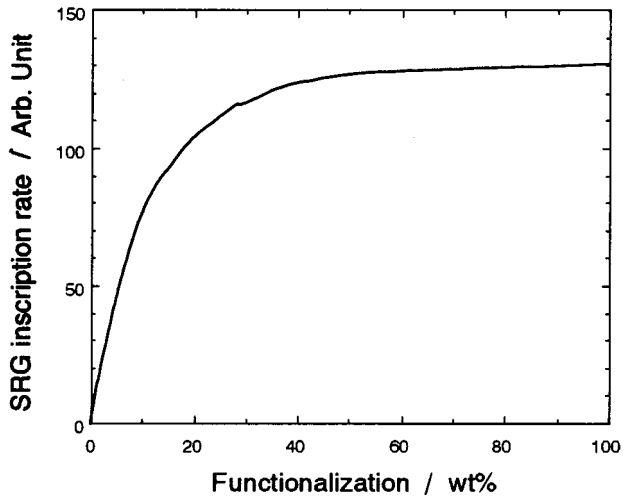

Figure 3. Theoretical calculation of functionalization dependence of the SRG inscription rate.

depth of the irradiated light should be different as a function of the azo functionalization. This kind of asymptotic tendency of the SRG inscription rate is predicted by the fluid mechanics model of Sumaru et al.,[16] as shown in Figure 3. The theoretical SRG inscription rate, $\partial h/\partial t$, is given by the following equation

$$\frac{\partial h}{\partial t} = \frac{-F_0 f(\alpha,h) \cos kx}{\mu}$$

$$f(\alpha,h) = \frac{k}{k^2-\alpha^2}\left[\frac{1}{\alpha} - \frac{\alpha}{k^2} - \frac{1}{\alpha}e^{-b} + \frac{2\alpha + ke^{-\alpha h}(e^{-kh} - e^{kh})}{k^2(e^{-kh} + e^{kh})}\right] \quad (1)$$

where the experimental parameters are defined as follows: the absorption coefficient $\alpha = \Phi \times 2.32 \times 10^{-1}$ μm^{-1} (Φ [wt %] is the functionalization), the film thickness h = 0.5 μm, the grating pitch Λ = 1.0 μm, and the wavenumber $k = 2\pi/\Lambda$. The force constant F_0 is proportional to the azo functionalization.

Although the solid line in Figure 3 explains the saturation tendency of SRG inscription rate for the azo functionalization qualitatively, there is a disagreement in the low functionalization region. The viscosity characteristics of either of the polymers at the molecular level are not well investigated yet. However, this disagreement presumably originates from the assumption that μ is constant, independent of the azo functionalization, because the azo chromophore acts as a plasticizer during light irradiation through trans−cis−trans photoisomerization. Above a certain chromophore concentration the polymer acts as a single component polymer system with a constant viscosity depending on such parameters as polymer rigidity. Below this chromophore concentration the polymer is a matrix analogous to a two-component polymer system with the viscosity strongly dependent on the extent and distribution of the components (in this case as if the azobenzene functionalized molecular component is dragging the rigid segment phase without the azo chromophore).[21,22] Further study for the dye functionalization dependence will be necessary to go beyond phenomenological observation.

Figure 4 shows the growth of diffraction efficiency of SRG on PMD78 film as a function of photon dose (= light intensity × irradiation time). Although the

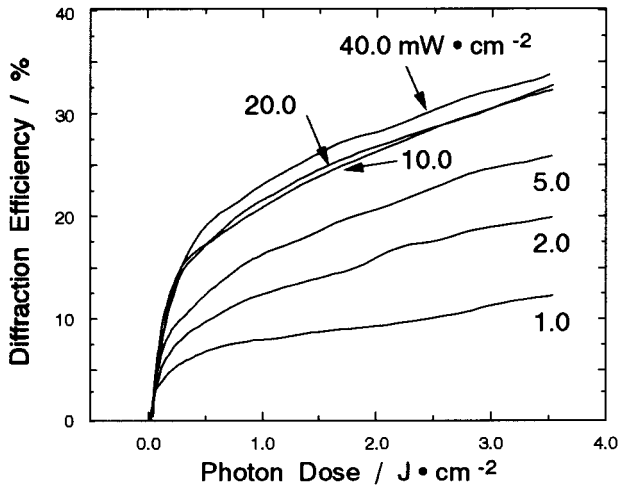

Figure 4. Intensity dependence of the SRG inscription rate on PMD78 film as a function of photon dose. The intensity of the exposed light was varied from 1 to 40 mW/cm^2. The film thickness was 400 nm.

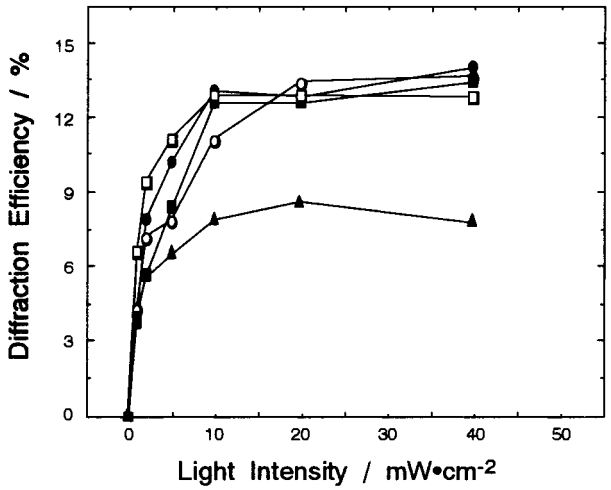

Figure 5. Intensity dependence of the SRG inscription rate for PMD with various functionalization. The diffraction efficiency proportional to the depth of surface modulation (vertical axis) was measured after the photoirradiation of 3.5 J/cm^2. Each symbol corresponds to the PMD functionalization and the film thickness as follows: ●, PMD78 (400 nm); ○, PMD76 (750 nm); ■, PMD72 (950 nm); □, PMD53 (1 μm); ▲, PMD39 (1 μm).

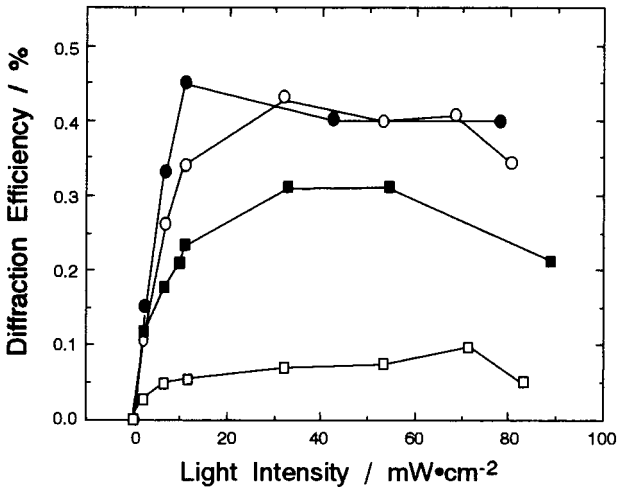

Figure 6. Intensity dependence of the SRG inscription rate for PMPD with various functionalizations. The diffraction efficiency (vertical axis) was measured after the photoirradiation of 4.0 J/cm^2. Each symbol corresponds to the PMPD functionalization as follows: ●, PMPD46; ○, PMPD40; ■, PMPD35; □, PMPD18. The film thickness of the films are 600−700 nm.

profiles of the diffraction efficiency map each other when the irradiated light intensity was stronger than ∼10 mW/cm^2,[3] it clearly decreases with decreasing the light intensity below ∼10 mW/cm^2. (It was found that the critical light intensity was independent of the spacing of the grating. Even further, it was confirmed that the SRG inscription rate did not go to zero even when the light intensity was below 0.1 mW/cm^2.) These results indicate that the velocity of the mass transport increases with increasing the irradiation light intensity, but it saturates at a certain point. In other words, the mass transport reaches the terminal velocity at around 10 mW/cm^2 in this system. The absolute value of the mass transport velocity may be determined as a balance of traction force caused by light irradiation and the friction (or restoring) force defined by the rheological properties of the polymer. Actually, at room temperature, the rate of SRG photofabrication in low-T_g (PMD) polymer is several tens of times faster than that of the high-T_g (PMPD) polymer. This is caused by the different rigidity of polymer main chain, which can affect the effective viscosity of the system. Meanwhile, from the microscopic viewpoint, the friction (or restoring) force may due to entanglement of the polymer chains and intermolecular interactions such as van der Waals interactions and dipolar interactions. Of course, these interactions are merely disrupted and overcome during the process of mass transport and reestablish. Therefore, the SRG inscription rate may vary dramatically in ionic azopolymers depending on the extent and nature of ionic complexation in the polymer films. It will be interesting to further investigate the critical threshold intensity in the ionic azopolymer systems.[23]

In the same way, the intensity dependence of SRG formation was examined on other PMD films with different degrees of functionalization. The results are shown in Figure 5 as a function of the light intensity. In all cases, a similar trend was observed, and the inscription rate was saturated around 10 mW/cm^2. This indicates that the degree of functionalization just determines the terminal velocity of the mass transport but does not affect the dynamics of photoactivated azobenzene chromophores.

The results of the same experiment performed on high-T_g (PMPD) polymers are shown in Figure 6. The tendency is almost the same as observed on PMD polymers, though the effective critical point was slightly shifted toward the higher light intensity side. (Although some decrease of the SRG inscription rate in higher light intensity region was observed, this is mainly due to photobleaching of azo chromophers.) It is rather surprising that the behavior is similar, since the PMPD polymers have significantly different T_g (difference of ∼90 °C at the maximum). The above results suggest that similar behavior can be expected despite differences in the nature of polymer main chain, as long as they have the same azo chromophores. From these results we can infer that the mechanical and the thermal properties of the bulk just influence the SRG inscription rate.

The dependence of the SRG inscription rate on the initial film thickness is given in Figure 7. The photon dose was fixed at 188 and 14 J/cm^2 for each PMPD46

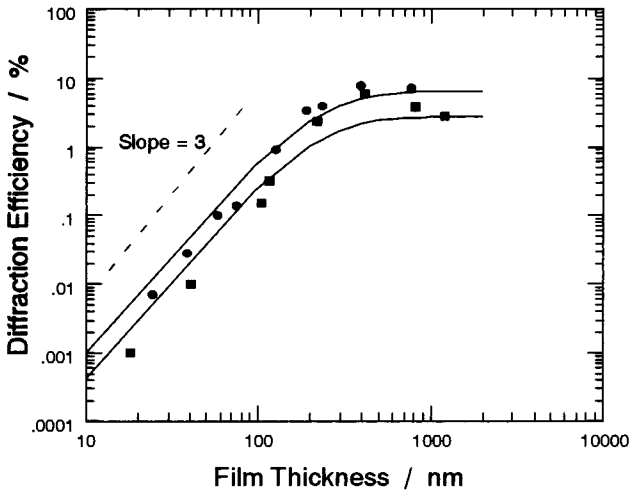

Figure 7. Film thickness dependence of the SRG inscription rate for PMPD46 (■) and PMD53 (●). The diffraction efficiency (vertical axis) was measured after the photoirradiation of 188 and 14 J/cm^2, respectively. The solid lines are the theoretical curves calculated by the fluid mechanics model in ref 14. The dashed line is the slope of three.

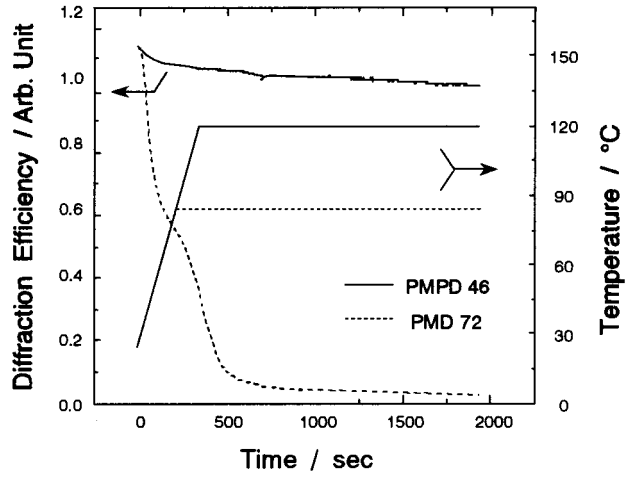

Figure 8. Thermal stability of the photofabricated SRG on high- and low-T_g polymer films (PMPD46 and PMD72). The solid and dashed lines indicate the diffraction efficiency (left axis) and temperature (right axis) for PMPD46 and PMD72, respectively. The speed of the heating process was approximately 0.5 °C/s.

and PMD53 film, respectively. As shown in the figure, a strong dependence of the SRG inscription rate on the initial film thickness is well explained by the theoretical curve derived from eq 1 through the entire range of the film thickness. Especially, according to eq 1, the thickness (h) dependence in the thin and the thick limit of the film can be derived as follows:

$$\lim_{b\to 0} f(b,c) = \frac{cb^3}{3} \propto h^3, \quad \lim_{b\to\infty} f(b,c) = \frac{1}{c} \qquad (2)$$

The fluid mechanics model[16] gives a cubic dependence in the small h region and the saturating tendency in the large h region and quantitatively describes these experimental data for both PMPD46 and PMD53.

Figure 8 shows the thermal stability of high- and low-T_g polymer (PMPD46 and PMD72). The SRG inscribed thin film was heated to the temperature lower than T_g by 50 °C (120 and 83 °C for PMPD46 and PMD72, respectively) at a rate of 0.5 °C/s and kept constant for

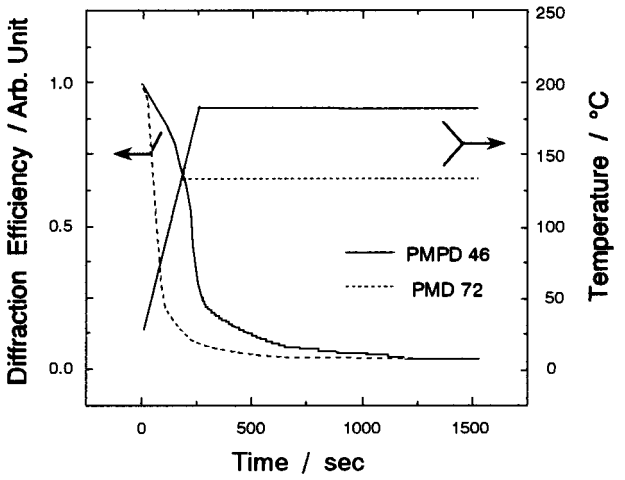

Figure 9. Thermal erasing characteristic of the photofabricated SRG on high- and low-T_g polymer films (PMPD46 and PMD72). The solid and dashed indicate the diffraction efficiency (left axis) and temperature (right axis) for PMPD46 and PMD72, respectively. The speed of the heating process was approximately 0.65 °C/s.

30 min. As shown in the figure, the high-T_g azo polymer could maintain the SRG profile well, whereas the low-T_g polymer (PMD72) showed considerable relaxation.

Homogeneous thermal heating above T_g was an effective way to erase the photofabricated SRG on azo polymers. The results for both polymers (PMPD46 and PMD72) are shown in Figure 9. The heating rate was 0.65 °C/s, and the film was kept at a temperature higher than T_g by 10 °C (180 and 143 °C for PMPD46 and PMD72, respectively) for 20 min. The diffraction efficiency dropped suddenly when the polymer film was heated just above the T_g. The SRG on PMPD46 disappeared within several tens of seconds, and that on PMD72 vanished within 10 s. The thermal erasing could be completed faster, just by keeping the sample at higher temperature. However, in that case, we have to take account of the thermal degradation of the azo chromophore as long as the experiment was performed under ambient conditions. Therefore, for practical applications, one has the choice of high-performance, high-T_g polymer depending upon the desired temperature stability of the device to be fabricated.

Conclusion

Photofabrication of SRG on two classes of polymers, with different degrees of azo functionalization, was investigated. By changing the main chain structure and the degree of azo functionalization, we could control the kinetics of the SRG photofabrication. As a result, a number of key insights into the microscopic deformation process for the SRG fabrication were established.

Several common features were observed in high-T_g (PMPD) and low-T_g (PMD) polymer systems, though the SRG formation rate was quite different. The SRG formation rate exhibited an S-shaped dependence on the azo functionalization in both polymers. The saturation tendency observed in the higher functionalization range was qualitatively explained by the fluid mechanics model proposed by Sumaru et al.; however, there still remained some disagreement, presumably due to the viscosity variation with change of azo functionalization.

It was found that the inscription rate of SRG saturates at a certain intensity (~10 mW/cm^2) of irradiated light in both polymer systems. This critical intensity was

not affected by either the degree of azo functionalization or the chemical structure, but the absolute value of the SRG inscription rate was strongly affected.

It should be noted that the SRG can be fabricated even on polymers with low degree of azo functionalization. This is quite interesting not only from an academic viewpoint but also for device applications. The dependence of the SRG formation rate on the initial film thickness is also explained by the formulation of the fluid mechanics model.

Thermal characteristics of the SRG on both polymer films were investigated. The photofabricated SRG on PMPD polymer was thermally stable at least up to 120 °C for 30 min due to its high-T_g characteristics. On the other hand, the photofabricated SRG on PMPD and PMD polymer could be erased quite easily just by heating above the T_g. These properties are promising for practical rewritable device applications.

Acknowledgment. The authors acknowledge Dr. Kimio Sumaru of National Institute of Materials and Chemical Research for helpful discussions. Tripathy and Kumar acknowledge financial support from NSF-DMR.

References and Notes

(1) Rochon, P.; Batalla, E.; Nathansohn, A. *Appl. Phys. Lett.* **1995**, *66*, 136−138.
(2) Kim, D. Y.; Li, L.; Kumar, J.; Tripathy, S. K. *Appl. Phys. Lett.* **1995**, *66*, 1166−1168.
(3) Kim, D. Y.; Li, L.; Jiang, X. L.; Shivshankar, V.; Kumar, J.; Tripathy, S. K. *Macromolecules* **1995**, *28*, 8835−8839.
(4) Barrett, C.; Natansohn, A.; Rochon, P. *J. Phys. Chem*. **1996**, *100*, 8836−8842.
(5) Ramanujam, P. S.; Holme, N. C. R.; Hvilsted, S. *Appl. Phys. Lett*. **1996**, *68*, 1329−1331.
(6) Holme, N. C. R.; Nikolova, L.; Ramanujam, P. S.; Hvilsted, S. *Appl. Phys. Lett*. **1997**, *70*, 1518−1520.
(7) Natanshon, A.; Rochon, P.; Ho, M. S.; Barrett, C. J. *Macromolecules* **1995**, *28*, 4179.
(8) Viswanathan, N. K.; Balasubramanian, S.; Li, L.; Kumar, J.; Tripathy, S. K. *J. Phys. Chem. B* **1998**, *102*, 6064−6070.
(9) Labarthet, F. L.; Buffeteau, T.; Sourisseau, C. *J. Phys. Chem. B* **1998**, *102*, 2654−2662.
(10) Bian, S.; Williams, J. M.; Kim, D. Y.; Li, L.; Balasubramanian, S.; Kumar, J.; Tripathy, S. K. *J. Appl. Phys.* **1999**, *86*, 4498−4508.
(11) Andruzzi, L.; Altomare, A.; Ciardelli, F.; Solaro, R.; Hvilsted, S.; Ramanujam, P. S. *Macromolecules* **1999**, *32*, 448−454.
(12) Ramanujam, P. S.; Pedersen, M.; Hvilsted, S. *Appl. Phys. Lett.* **1999**, *74*, 3227−3229.
(13) Kumar, J.; Li, L.; Jiang, X. L.; Kim, D. Y.; Lee, T. S.; Tripathy, S. K. *Appl. Phys. Lett*. **1998**, *72*, 2096−2098.
(14) Barrett, C. J.; Rochon, P. L.; Natansohn, A. L *J. Chem. Phys.* **1998**, *109*, 1505−1516.
(15) Pedersen, T. G.; Johansen, P. M.; Holme, N. C. R.; Ramanujam, P. S.; Hvilsted, S. *Phys. Rev. Lett.* **1998**, *80*, 89−92.
(16) Sumaru, K.; Yamanaka, T.; Fukuda, T.; Matsuda, H. *Appl. Phys. Lett.* **1999**, *75*, 1878−1880.
(17) Xie, S.; Natansohn, A.; Rochon, P. *Macromolecules* **1994**, *27*, 1489−1492.
(18) Fukuda, T.; Matsuda, H.; Viswanathan, N. K.; Tripathy, S.; Kumar, J.; Shiraga, T.; Kato, M.; Nakanishi, H. *Synth. Met.* **1999**, *102*, 1435−1436.
(19) Kato, M.; Shiraga, T.; Fukuda, T.; Matsuda, H.; Nakanishi, H. *J. Photopolym. Sci. Technol.* **1998**, *11*, 161−162.
(20) Natanshon, A.; Rochon, P.; Gosselin, J.; Xie, S. *Macromolecules* **1992**, *25*, 2268−2273.
(21) Fujino, K.; Ogawa, Y.; Kawai, H. *J. Appl. Polym. Sci.* **1964**, *8*, 2147−2161.
(22) Horino, T.; Ogawa, Y.; Soen, T.; Kawai, H. *J. Appl. Polym. Sci.* **1965**, *9*, 2261−2272.
(23) Tripathy, S. K.; et al., submitted to *Macromolecules*.

MA991803D